energies

MDPI

Article

DC Bus Voltage Selection for a Grid-Connected Low-Voltage DC Residential Nanogrid Using Real Data with Modified Load Profiles

Saeed Habibi *, Ramin Rahimi, Mehdi Ferdowsi and Pourya Shamsi

Electrical and Computer Engineering, Missouri University of Science and Technology, Rolla, MO 65401, USA; R.rahimi@mst.edu (R.R.); Ferdowsi@mst.edu (M.F.); Shamsip@mst.edu (P.S.)
* Correspondence: S.habibi@mst.edu

Abstract: This study examines various low voltage levels applied to a direct current residential nanogrid (DC-RNG) with respect to the efficiency and component cost of the system. Due to the significant increase in DC-compatible loads, on-site Photovoltaic (PV) generation, and local battery storage, DC distribution has gained considerable attention in buildings. To provide an accurate evaluation of the DC-RNG's efficiency and component cost, a one-year load profile of a conventional AC-powered house is considered, and AC appliances' load profiles are scaled to their equivalent available DC appliances. Based on the modified load profiles, proper wiring schemes, converters, and protection devices are chosen to construct a DC-RNG. The constructed DC-RNG is modeled in MATLAB software and simulations are completed to evaluate the efficiency of each LVDC level. Four LVDC levels—24 V, 48 V, 60 V, and 120 V—are chosen to evaluate the DC-RNG's efficiency and component cost. Additionally, impacts of adding a battery energy storage unit on the DC-RNG's efficiency are studied. The results indicate that 60 V battery-less DC-RNG is the most efficient one; however, when batteries are added to the DC-RNG, the 48 V DC distribution becomes the most efficient and cost-effective option.

Keywords: direct current (DC) distribution; residential nanogrid (RNG); DC–DC converter; efficiency; DC appliance

Citation: Habibi, S.; Rahimi, R.; Ferdowsi, M.; Shamsi, P. DC Bus Voltage Selection for a Grid-Connected Low-Voltage DC Residential Nanogrid Using Real Data with Modified Load Profiles. *Energies* **2021**, *14*, 7001. https://doi.org/10.3390/en14217001

Academic Editors: Laura Ramírez Elizondo and Aditya Shekhar

Received: 25 September 2021
Accepted: 20 October 2021
Published: 26 October 2021

1. Introduction

In the last decade, direct current (DC) power distribution research has become popular in commercial and residential facilities due to the developments in internally DC loads—such as electronics and variable frequency drives, the widespread implementation of roof-top photovoltaic (PV) systems, and battery use [1–3]. DC distribution may be more energy efficient than AC distribution in data centers and commercial buildings [4], although implementing DC distribution in residential buildings necessitates further research and development in terms of distribution voltage level and load compatibility [5,6]. Compared to data centers and commercial facilities, the residential sector saves less electricity due to lower load power consumption and lower time of use coincidence between on-site renewable energy sources (RESs) power generation and demand [7,8], while ongoing research on DC houses and buildings in the residential sector depicted that DC power distribution is more efficient than AC alongside energy and cost savings; it is estimated that there are 14% and 5% total electricity savings in DC-powered residences with and without energy storage, respectively [9]. Additionally, a study about a DC residential nanogrid (DC-RNG) consisting of PV generation and energy storage indicated that the baseline energy consumption and emissions of these homes were reduced by 7–16% [1]. A recent publication compared office buildings with AC and DC distribution, and its results depicted that the DC distribution in an office building presented higher efficiency in low grid energy exchange and high electric vehicle demand [10].

Due to the lack of standardization for DC distribution voltage, a variety of DC voltage levels are suggested in the literature. A DC distribution network ranging from high voltage

(100 kV) to extra low voltage (24 V) is suggested in [11]. With the integration of distributed power generation into the DC distribution network, the authors attempted to demonstrate a scalable framework for future urban power supply. Based on the market and technical characteristics, a DC voltage level of less than 48 V for applications such as lighting and electronics with a power range up to 1 kW, a DC voltage level in the range of 60–230 V for household and office loads with a power range up to tens of kW, and 350–450 V DC as the main voltage for residential and commercial building distribution are offered in [12]. Based on a device power and its application, a voltage range of 24–48 V DC for low power loads, such as electronic equipment with a power range up to 400 W, 230–400 V DC for kitchen and laundry rooms with a power range of 0.4–10 kW, and more than 538 V DC for applications with a power range more than 10 kW are offered in [13]. All aforementioned studies offered DC distribution voltage levels based on the power ratings of appliances and application types. Other researchers have conducted deeper investigations of DC distribution voltage selection. Using conventional building wiring, 326 V DC was offered for the distribution voltage level, considering only voltage drops and wiring losses [14]. Additionally, the DC bus voltage levels are investigated in a standalone DC-RNG in [15]; the investigated DC voltages levels were 12 V, 24 V, 48 V, 60 V, and 100 V, and the efficiency of the nanogrid was calculated at each voltage level along with the cost of implementation. Regarding performance, the authors considered voltage drops, power losses, and maximum allowable cable length, and they revealed that 100 V yielded the best performance. Taking cost and performance into account, 48 V DC was the best choice. A 72 V distribution voltage was considered for a standalone DC-RNG up to 250 W in [16] for a limited number of loads. Previous research in this field suffered from simplifying assumptions, like considering static system operating points, and as the authors mentioned in [17], the lack of realistic data, such as load and generation profiles, and converter efficiency curves that prevent accurate results. Realistic data for load and generation, converter efficiency curves, and wiring models for small and medium commercial buildings were used in [2]. The authors showed that a medium office building with a DC distribution system was the best-case scenario and offered 18.5% energy savings compared to its AC counterpart, when the load profiles of conventional AC appliances were used.

Most of the loads in residential and commercial buildings are internally DC, thus meaning that conventional loads—including electronics, light emitting diode (LED) lighting, and variable speed drives—use rectifier stages to convert AC voltage to DC voltage. Eliminating the AC to DC conversion will yield more efficient systems [18]. There are not market-ready DC loads for every application in the residential sector, but in [19], the authors modified loads (such as motor loads, electronics, and lighting) to leverage DC input and improve efficiency. In off-grid applications, energy is directly supplied by PV or battery, thus making more DC appliances available. The authors in [5] conducted a survey on DC-ready appliances that included heating ventilation air condition (HVAC), electronics, refrigeration, and lighting.

This study develops a simulation model for an accurate efficiency assessment and component cost evaluation of a DC-RNG, considering the aforementioned limitations in previously published papers. In this paper, realistic annual data for loads and PV generation are used, taking into account the effects of various weather conditions. To further increase the accuracy of the efficiency assessment and financial analysis, the AC load profiles are modified to DC load profiles, and by using the modified load profiles, a DC-RNG is constructed. Cable sizes, converter ratings, PV, and battery capacities are determined by the modified load profile. Furthermore, accounting for the wiring loss, a detailed wiring diagram is considered for distribution in the DC-RNG. The efficiency and component cost of the DC-RNG is evaluated for four different LVDC levels of 24 V, 48 V, 60 V, and 120 V without and with energy storage

The rest of this paper is organized as follows: Section 2 introduces the DC-RNG structure and its components—including loads, converters, PV, and battery storage. Section 3 presents the floor plan of the house and equivalent wiring resistance for each load category.

Section 4 provides the simulation procedure for the efficiency evaluation, and Sections 5 and 6 include the component cost, simulation results and discussion, respectively. Finally, the conclusion is presented in Section 7.

2. DC-RNG Structure and Components

Different DC distribution topologies for a DC nanogrid are categorized in [3,20]; the unipolar topology is preferred in houses with low power consumption. In this study, the DC-RNG is defined as the internal network of a two-bedroom house; its structure and components are shown in Figure 1. As presented, the loads of the DC-RNG are connected to the DC bus through proper DC–DC converters, and the DC bus is connected to the AC grid through a bidirectional AC–DC converter. Four LVDC levels, including 24 V, 48 V, 60 V, and 120 V, are investigated for DC bus voltage in the nanogrid with only PV generation (DC-RNG$_{PV}$) and in a nanogrid with PV generation and battery storage (DC-RNG$_{PV\text{-}B}$).

The main components of the DC-RNG are loads, converters, PV, and battery bank. The DC-RNG's load is a modified version of an AC load profile—the AC load profile is provided by the National Renewable Energy Laboratory and measured in the state of Florida [21]. The modified load profile presents the annual load profile of the DC-RNG with one-hour sample time. Based on the modified load profiles, proper converters, PV size, and battery capacity are chosen for the DC-RNG.

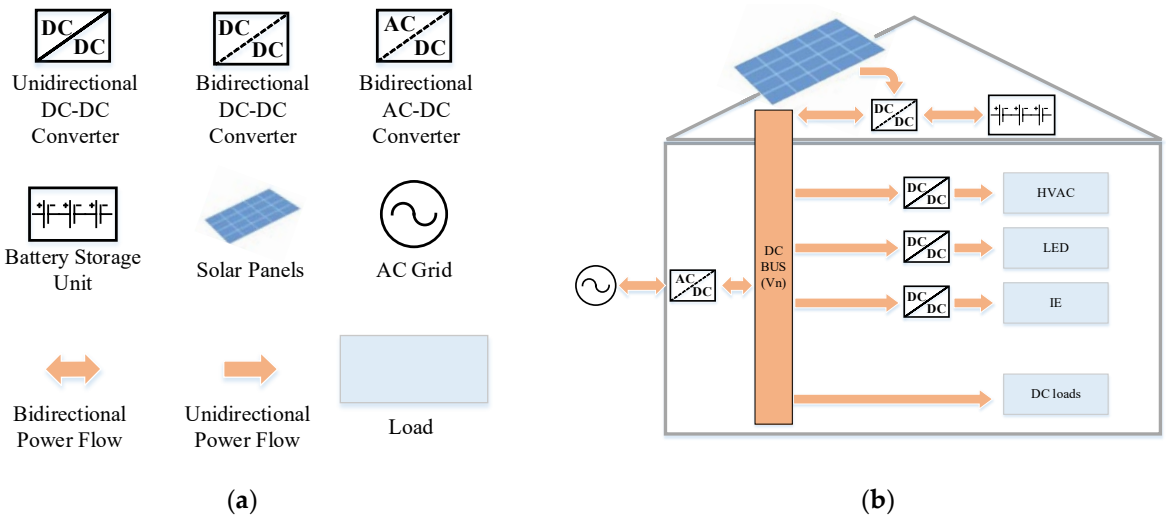

Figure 1. DC-RNG structure and components: (**a**) symbol guide, (**b**) structure.

2.1. Loads

Loads are categorized into four types: heat ventilation air conditioning (HVAC), lighting, interior equipment (IE), and water heating. Unlike AC, DC appliances are not available for every residential application. Most of the DC-ready appliances are for off-grid applications. In this study, the latest available DC-ready appliances are used to construct a DC-RNG [5,22]

Determining a DC-RNG load profile on the basis of the available AC load profiles requires modifications on the AC load profiles. In this section, a load scaling scheme is used that scales the AC appliance's load profile to an equivalent DC appliance load profile. For each load category, a conventional AC appliance, based on the Building Characteristics for Residential Hourly Load Data [21], is considered. Then, an equivalent DC appliance with the same performance characteristics is chosen. For example, the DC HVAC with the same cooling and heating capacity as the AC HVAC is chosen. The ratio of the DC appliance rated power to the AC appliance rated power is the scaling factor. The scaling factor for each category of loads is calculated using the rated powers of the DC and AC appliances, then the scaling factor is applied to the load profile throughout the data. The average modified load profiles are shown in Figure A1 in Appendix A for each category of load.

2.1.1. Lighting

The lighting technology used in the Residential Hourly Load Data is compact fluorescent lamps (CFL). Replacement of CFLs with other technologies, like light emitting diodes (LEDs), has been investigated. Using LED lighting technology has been proved to be more efficient than CFL lighting [23], and LEDs are more compatible with DC technology compared to CFLs [24]. The lighting power consumption profile is scaled from conventional CFLs to LEDs. At any given lumens, LED lighting requires 0.65 of CFL power on average [24].

2.1.2. HVAC

Based on the Building Characteristics for Residential Hourly Load Data in hot-humid climates, the air conditioner efficiency rating met the SEER 16 standard. Therefore, for the selected data in a hot–humid climate, an HVAC system with 24,000 BTU cooling/heating capacity is suitable [25]. Selected AC and equivalent DC HVAC systems are presented in Table A1 in Appendix A. Based on Table A1, the scaling factor for the HVAC load profile is 0.67.

2.1.3. Water Heater

DC water heaters are not available on the market; however, DC water heating elements are available in 12 V, 24 V, and 48 V at up to 2000 W [26]. Considering that water heater elements are easily manufactured at any DC low voltage and their power ratings can be customized, it is assumed that DC water heaters will be available in the future. In this research, the water heater load profile is not scaled, and it is assumed that the water heaters could be connected directly to the DC bus.

2.1.4. Interior Equipment

Among interior equipment, DC refrigerators/freezers are available on the market, and refrigerators/freezers are the primary power consumers in this category. Other interior equipment—including fans, griddles, microwaves, blenders, heaters, and hair dryers—are available in 12 V and are designed to operate on car batteries [22]. Excluding each device's power consumption profile from the IE load profile requires a complicated method; accordingly, for simplicity, a fraction of IE load power is considered to be the refrigerator/freezer power, and only a fraction of IE load power is scaled. Due to the unavailability of other DC-powered equipment in this category, it is assumed that all the other equipment, e.g., kitchen oven and washer/dryer, could operate using different DC voltage levels. This assumption is made to avoid biased results at specific voltages. As presented in Appendix A, the AC refrigerator approximately consumes 1.5 times more power than its DC counterpart.

2.2. Converters

DC market-ready appliances are mostly available in 24 V and 48 V; therefore, voltage conversion stages are needed for loads when constructing a DC-NRG with existing DC appliances. LED drivers, AC–DC converters, and MPPT charge controllers (CC) are needed at each DC bus voltage. Loads that operate at the DC bus voltage do not require DC–DC converters to connect to the DC bus. At each DC-RNG, the power converters are selected on the basis of the voltage and power ratings. These converters are available on the market, and the efficiency curves of the converters are employed in the simulation. The efficiency curves of the converters are shown in Figure A2 in Appendix B. The converters that are used in this study are described as follows:

- The DC–DC converters provide proper voltage levels to loads from the DC bus voltage. These converters are chosen based on the required voltage and power ratings at each voltage level and application. Enough number of converters are paralleled to meet load power demands. The selected converters are available on the market, and their efficiency curves can be found on the manufacturers' datasheets.

- The MPPT CC conditions PV panel power at the maximum power point, and it controls the charging and discharging of the battery bank. The chosen battery bank voltage is the same as DC bus voltage, and battery bank voltage is assumed to be constant during charging and discharging. Therefore, only the MPPT CC handles the battery charging and discharging, and additional converter is not required.
- The AC–DC bidirectional converter is an interface converter between the AC grid and the DC-RNG. This converter absorbs power from and injects power to the grid. During peak load times, power flows from the grid to the DC-RNG; during high PV power generation, if the battery is fully charged, excess PV power flows to the AC grid through the AC–DC converter.

2.3. PV Generation

The annual PV generation profile adopted from an existing PV plant that was geographically close to the house. The PV plant data have a one-hour sampling time, the same as the load profile sampling time. The inclusion of various weather conditions in the simulation results is ensured by using an annual PV generation profile [27]. Based on the net zero energy (NZE) building definition, the total amount of energy used by the building on an annual basis is equal to the amount of renewable energy created on the site. Therefore, the original data from the PV plant was scaled to provide the DC-RNG's PV power generation capacity for the simulation. The PV system capacity for the DC-RNG is obtained by matching the annual values of the generated and consumed energy. In (1), p_i^{load} and p_i^{pv} represent the DC-RNG's load power and the PV plant power at i instance, respectively. k is the scaling factor for the PV plant power. By integrating the load power and the PV plant power over a year and using (2), k is calculated. That is, the scaling factor applied to the original PV plant capacity to obtain appropriate PV capacity for the DC-RNG. By applying this procedure on the DC-RNG load data and the PV plant data, 3150 W is obtained for the solar capacity. The annual PV generation profile is shown in Figure A3 in Appendix C.

$$\sum_i p_i^{load} = \left(\frac{1}{k}\right) \sum_i p_i^{pv} \tag{1}$$

$$k = \frac{\sum_i p_i^{pv}}{\sum_i p_i^{load}} \tag{2}$$

2.4. Battery Storage

A battery energy storage system is a critical part of a stand-alone system, because it stores energy during days and supplies loads at nights. Unlike stand-alone systems, grid-connected systems use battery storage for lowering power grid reliance and minimizing energy loss, while using an on-site renewable generation. In an ideal condition, an energy storage system could store all excess power provided by PV over the course of a year, but selecting a battery with such a large capacity could result in large amounts of unused capacity. Therefore, small capacities for grid-connected systems are more suitable. Using the chosen PV capacity, simulations are performed to identify the battery storage capacity for the DC-RNG. Based on the method described in [28], the DC-RNG's efficiency and the battery down time (BDT) for 24 V DC-RNG by sweeping battery capacity from 2.4 kWh to 48 kWh are shown in Figure A4 in Appendix C. The number of hours in one year that batteries are disconnected due to a low state of charge is represented by BDT [28]. According to Figure A4, a battery storage unit with a capacity of 24 kWh provides high efficiency and low BDT. Choosing larger capacities do not result in considerable improvement in the efficiency and BDT.

The battery storage charging mechanism uses a simple algorithm. The battery is charged only when PV power is more than the load power, and it is discharged when the load power exceeds the PV-generated power [2]. The battery storage is directly connected

to the DC bus and its voltage is considered to be fixed with negligible changes during charge and discharge processes.

Using 20 conventional Lead–Acid 12 V-100 Ah batteries, the configuration for each voltage level is achieved. Figure 2 shows the configuration of the battery storage unit, where N_s represents the number of batteries connected in series in each branch and N_p is the number of battery branches connected in parallel. Using N_s and N_p, the maximum allowable charging and discharging current, the short circuit current, and rated breaking capacity of protection devices are found.

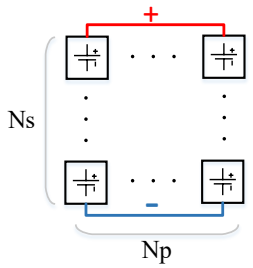

Figure 2. Battery storage unit configuration.

3. Floor Plan and Wiring Resistance

To obtain an accurate estimation of wiring loss, the wiring length and wiring size are required to calculate the wiring resistance. Using the wiring resistance and the current passing through the circuit, the wiring loss is calculated at each instance. A floor plan with 94 m^2 area is considered for the DC-RNG based on the Building Characteristics for Residential Hourly Load Data [21]. The floor plan, appliance placement, wiring diagram, and dimensions are shown in Figure 3. Based on the diagram, the wiring length for each category of loads is determined geometrically. Using (3), the wiring resistance (R_i) of i^{th} load is found. In this equation, A_i and l_i are the cross-sectional area and length of the wire, respectively. In (3), ρ is the specific resistance of the conductive material.

$$R_i = \frac{\rho l_i}{A_i} \tag{3}$$

Assuming that one load category includes N different items, and that each of these items consumes equal power, by using (4) and (5), the wiring loss and equivalent resistance of each category of loads are calculated. Therefore, by knowing the number of items in each load category and the resistance of each load's circuit, the equivalent wiring resistance is calculated. The wire cross-sectional area is identified based on the maximum current passing through the circuit; however, based on the National Electric Code (NEC), regardless of peak current, the minimum wire size is 12 AWG for the residential wiring [2]. The equivalent resistance for each load category is listed in Table 1.

$$P_{loss} = \sum_{i=1}^{N} R_i \left(\frac{I}{N}\right)^2 = \sum_{i=1}^{N} \left(\frac{R_i}{N^2}\right) I^2 \tag{4}$$

$$R_{eq} = \sum_{i=1}^{N} \left(\frac{R_i}{N^2}\right) \tag{5}$$

Table 1. Equivalent resistance of each category of loads for different voltage levels.

Load	Equivalent Resistance (mΩ)			
	24 V	**48 V**	**60 V**	**120 V**
HVAC	5.961	15.071	23.959	23.959
Lighting	16.641	16.641	16.641	16.641

Table 1. *Cont.*

Load	Equivalent Resistance (mΩ)			
	24 V	**48 V**	**60 V**	**120 V**
IE	57.063	57.063	57.063	57.063
Water Heater	0.327	5.212	10.458	26.436
MPPT CC	26.436	26.436	26.436	26.436

4. Efficiency Calculation

Power losses are categorized into three types: converters loss, wiring loss, and battery chemical loss. To accurately evaluate the DC-RNG's energy efficiency, components contributing to power loss are modeled, and an hourly modified load profile as well as the hourly scaled PV generation data are used to calculate power losses in the wires, converters, and batteries.

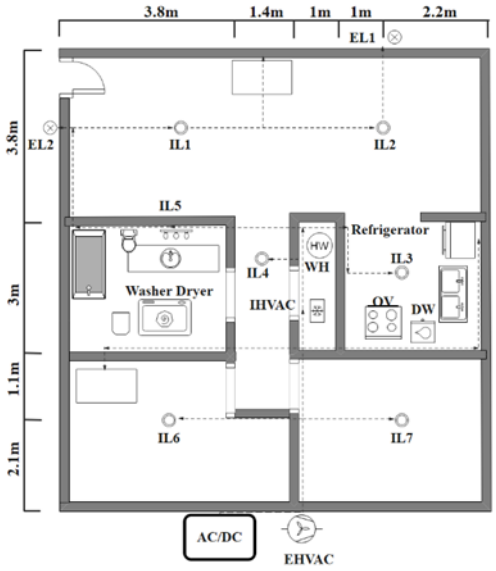

Figure 3. House floor plan and wiring diagram.

The power passing through a converter varies based on load power. To calculate converter power losses (6)–(9) are used. In (6)–(9), p_i^l represents the power of l^{th} load at i^{th} instance, η_i^c represents c^{th} converter's efficiency at i^{th} instance with p_i^l passing through it. Using (7), power loss of a converter at i^{th} instance ($p_{loss}^c i$) is calculated. P_{loss}^c is power loss associated with a converter through all samples, and P_{CL} represents the total power loss of converters in the DC-RNG. The number of data samples during a year is N_d and the number of the converters in the DC-RNG is N_c.

$$\eta_i^c\left(p_i^l\right) = \frac{p_i^l}{p_i^l + p_{loss}^c i} \tag{6}$$

$$p_{loss}^c i = p_i^l\left(1 - \frac{1}{\eta_i^c\left(p_i^l\right)}\right) \tag{7}$$

$$P_{loss}^c = \sum_{i=1}^{N_d} p_{loss}^c i \tag{8}$$

$$P_{CL} = \sum_{c=1}^{N_c}\sum_{i=1}^{N_d} p_{loss}^c i = \sum_{c=1}^{N_c} P_{loss}^c \tag{9}$$

The wiring power loss is calculated using (10)–(12). In (10)–(12), $p^{w}_{loss_i}$ represents wiring power loss of w^{th} circuit, which connects to the l^{th} load category through c^{th} converter at i^{th} instance, and P^{w}_{loss}, P_{WL}, and N_l are wiring power loss of w^{th} circuit throughout all data samples, total wiring power loss, and number of circuits, respectively.

$$p^{w}_{loss_i} = R_{eqi}\left(\frac{p^{l}_{i} + p^{c}_{loss\,i}}{V_n}\right)^2 \tag{10}$$

$$P^{w}_{loss} = \sum_{i=1}^{N_l} p^{w}_{loss_i} \tag{11}$$

$$P_{WL} = \sum_{c=1}^{N_l}\sum_{i=1}^{N_d} p^{w}_{loss_i} = \sum_{c=1}^{N_l} P^{w}_{loss} \tag{12}$$

The chemical power loss is calculated as a percentage of the energy delivered to and absorbed from batteries. According to [2], the chemical loss of batteries is about 19% of its rated capacity for a round-trip. The standing loss of batteries is assumed to be negligible for a one-year simulation timeframe.

The simulation flow diagram, shown in Figure 4, starts with importing data to MATLAB software, then the profile of each load category is modified using the scaling factors from Section 2.1. After modifying the load profiles, simulation parameters—such as DC bus voltage (V_n), battery nominal capacity (C_n), converters' efficiency curve, and wiring data—are initialized, and then the number of required parallel converters and PV size are determined. After completing the previous steps, the simulation of the DC-RNG starts by determining the amount of energy stored in the battery and the amount of energy transferred between the grid and the DC-RNG, using the total load power and PV power at each step. The power loss of elements (converters, wires, and battery) is computed using each category's load profile during these calculations.

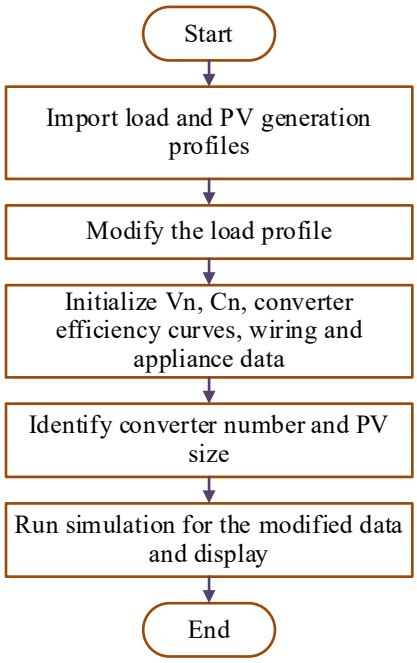

Figure 4. Flow diagram of simulation process.

5. Component Cost

Different converters and wire sizes are used to evaluate the efficiency of the DC-RNG at each LVDC level; therefore, the cost of components is important when comparing different voltage levels for a DC-RNG. In addition, constructing a DC-RNG requires appropriate

protection devices with respect to voltage levels. Circuit breaker selection factors—such as short circuit capacity, rated current, and voltage—differ from one voltage level to another; due to these differences, the cost of converters, cables, and protection devices are considered in this study.

5.1. Converter

The AC–DC converter, MPPT CC, and LED drivers are required at each voltage level. As presented in Table 2, a market-ready converter is selected for each application in the DC-RNG. Based on the power rating required for the application, enough number of converters are paralleled to meet the power rating requirement. Some selected DC appliances do not require DC–DC converters; for example, the HVAC unit operates at 48 V and 60 V DC without using a DC–DC converter, that is, the HVAC unit is directly connected to the DC bus at 48 V and 60 V; however, it is connected to the 24 V or 120 V DC bus through a DC–DC converter.

The total converter cost for 48 V is less than other voltage levels. The total converter cost for 24 V and 60 V DC-RNGs are close and less than 120 V DC-RNG. 120 V DC-RNG converter cost is more than twice that of 48 V DC-RNG.

5.2. Cable

For conducting wire cross-sectional and length calculations, the number of circuits in the DC-RNG must be determined. In this study, different circuits were assumed for each room and each high-power appliance. By taking the power of each load from Section 2, and by using the maximum allowable current for each size of wire, the cross-sectional area of each circuit's wire was determined. In Table 3, the primary cable size for wiring the DC-RNG is AWG 12, and at lower voltages, larger cable sizes are required for the HVAC unit, water heater, and PV. Lower voltages necessitate larger cables; consequently, cable costs are greater at lower voltages.

5.3. Protection

Due to the wide range of voltage levels and grounding techniques in DC systems, selecting protection devices is challenging. Additionally, the absence of natural zero crossings and high *di/dt* makes it more difficult. There are two types of faults in a DC-RNG: short-circuit (SC) and open-circuit (OC). The OC fault is considered more of a control issue than protection; therefore, in this paper, only protection against SC faults is considered. As shown in Figure 5, the SC fault could happen between the positive and negative polarities of the DC bus (F1), or it could occur between the positive polarity and the ground (F2). Using proper circuit breakers for each circuit provides protection against F1 and F2 faults [23].

To design a reliable protection scheme for a system, the inrush load current, the installation point short-circuit capacity (I_{sc}), device nominal power (P_n), and voltage level (V_n) must be considered. In DC systems, inrush load currents are lower than those in AC systems [29]; thus, in this paper, only I_{sc}, P_n, and V_n are considered.

To estimate circuit breaker cost for the DC-RNG, as presented in Table 4, circuit breakers are considered for the kitchen, living room, bedrooms, bathroom, and high-power appliances, such as HVAC and water heater, battery bank, and one main circuit breaker for the DC-RNG. In a conventional house's protection, circuit breakers are dedicated to the refrigerator, dishwasher, microwave, and electric range circuits in the kitchen. Although specific DC appliances are not chosen for these loads in this paper, four different circuit breakers with the same current ratings are selected for the kitchen circuit to evaluate the protection cost accurately.

The current ratings of the circuit breakers are chosen based on 125% of the load rated current for the selected loads in Section 2.1. For the other breakers, which specific appliances are not chosen, the DC equivalent of a conventional AC circuit breaker at 120 V AC is chosen. The conventional current rating for an AC circuit breaker is 40 A for kitchen,

30 A for bathroom, 20 A living room, and 15 A for each bedroom. The rated battery circuit breaker current is based on the maximum allowable charging and discharging current.

Table 2. Converters, their prices, and total converter cost at each voltage level.

Converter	Voltage Level (V)	24	48	60	120
AC–DC	Model	LCM3000Q-T	LCM3000W-T	CP3000/3500A	HEP-1000-100
	Unit price ($)	652.93	652.93	761.27	422.25
	Required No.	2	2	2	6
MPPT Charge Controller	Model	XTRA4415N	XTRA4415N	TS-MPPT-60-600V-48	SRXHV 300/30
	Unit price ($)	249.99	249.99	1009.95	809
	Required No.	2	2	1	1
HVAC	Model	CFB600-24S48	-	-	DDR-480D-48
	Unit price ($)	232.30	-	-	191.52
	Required No.	5	-	-	5
LED Driver	Model	LDD-700L	LDD-700H- DA	LDD-600H	PLC-30-15
	Unit price ($)	3.15	11.41	4.39	22.43
	Required No.	9	9	9	9
IE	Model	-	CQB150W	CHB150	CHB150
	Unit price ($)	-	174.52	150.00	150.00
	Required No.	-	1	1	1
Total converter cost ($)		2979.49	2083.05	2722.00	4651.97

Table 3. Wire size, length, and total wire cost at each voltage level.

Voltage Level (V)	Estimated Wire Length						Total Wire Cost ($)
	AWG 12 (m)	AWG 10 (m)	AWG 6 (m)	AWG 2 (m)	AWG 2/0 (m)	AWG 4/0 (m)	
24	357.4	0	38.8	0	0	20.4	669.65
48	357.4	18.8	20.4	0	20.4	0	517.49
60	376.2	0	20.4	20.4	0	0	432.91
120	376.2	0	40.8	0	0	0	353.93

I_{sc} of each circuit is determined using (13), in which V_n is the DC voltage level and R_{dc} is the resistance of each circuit. The short circuit capacity of the battery bank (I_{scb}) is calculated using (14), which R_b is the battery internal resistance. An AMG battery 12 V 100Ah with an internal resistance of 5 mΩ is chosen [30]. For battery protection, polarized circuit breakers could not be used because the battery current flows in both directions when charging and discharging.

$$I_{sc} = \frac{V_n}{R_{dc}} \tag{13}$$

$$I_{scb} = \frac{V_n}{\left(\frac{N_S R_b}{N_p}\right)} \tag{14}$$

There are two types of connections for a circuit breaker with more than one pole: series and parallel; series connection of poles is suitable for high-voltage applications, and parallel connection of poles has better performance in low-voltage high-current applications. Due to the low-voltage distribution in the DC-RNG, parallel connection of poles could be used for the protection scheme. Two parallel poles can be used up to 1.6 times of the DC

breaker's rated current, and three parallel poles can be used up to 2.25 times of the DC circuit breaker's current rating [29].

The circuit breakers cost for each voltage level is presented in Table 4. The cost of circuit breakers at the lowest voltage is much higher than at other voltage levels, and the total circuit breakers' cost decreases as voltage level increases. Higher circuit breaker cost at low voltages is because of high I_{sc}, low R_{dc}, and high rated current of breakers. DC circuit breakers are generally intended for DC voltages beyond 120 V or 220 V, therefore, the rated voltage of the circuit breaker has no influence on the total cost. In this research, the market-ready circuit breakers are used for the low-voltage DC-RNG, therefore only the short circuit current and rated current are influential on the total circuit breaker cost.

Table 4. Circuit breakers and their cost.

DC Bus Voltage (V)	24		48		60		120	
Circuit Breaker	**Product ID**	**Price ($)**	**Product ID**	**Price ($)**	**Product ID**	**Price ($)**	**Product ID**	**Price ($)**
Kitchen	1SDA068092R1	813.65	1SDA066808R1	196.82	1SDA066807R1	166.53	1SDA066804R1	133.64
Room 1	1SDA066807R1	166.53	1SDA066804R1	133.64	1SDA066803R1	133.12	1SDA066800R1	131.55
Room 2	1SDA066807R1	166.53	1SDA066804R1	133.64	1SDA066803R1	133.12	1SDA066800R1	131.55
Living Room	1SDA066808R1	196.82	1SDA066805R1	134.77	1SDA066804R1	133.64	1SDA066801R1	130.52
HVAC	1SDA066807R1	166.53	1SDA066804R1	133.64	1SDA066803R1	133.12	1SDA066801R1	130.52
Water Heater	1SDA100566R1	1379.78	1SDA066806R1	252.68	1SDA066808R1	196.82	1SDA066805R1	134.77
Bathroom	1SDA068058R1	627.66	1SDA066807R1	166.53	1SDA066806R1	157.91	1SDA066803R1	133.12
Battery	1SDA067020R1	427.01	1SDA066809R1	252.68	1SDA066808R1	196.82	1SDA066805R1	135.21
Main Circuit Breaker	1SDA100762R1	2671.64	1SDA100416R1	1499.59	1SDA100415R1	1272.97	1SDA068059R1	738.22
Total Price ($)	9057.10		3494.45		3023.64		2200.02	

As shown in Figure 6, the total component cost for 24 V DC-RNG and 48 V DC-RNG implementations are the highest and lowest, respectively. The protection cost contributes the most to the total cost at 24 V and 48 V DC-RNGs. Compared to 24 V DC-RNG, the converter, cable, and protection costs drop for 48 V DC-RNG.

By increasing DC bus voltage to 60 V, the protection and cable cost decrease, and the converter cost increases. The total component cost at 60 V is slightly higher than 48 V. The protection and cable cost at 120 V are lower than other voltage levels, but due to the high converter cost, the total component cost at this voltage level is higher than 48 V and 60 V DC-RNGs.

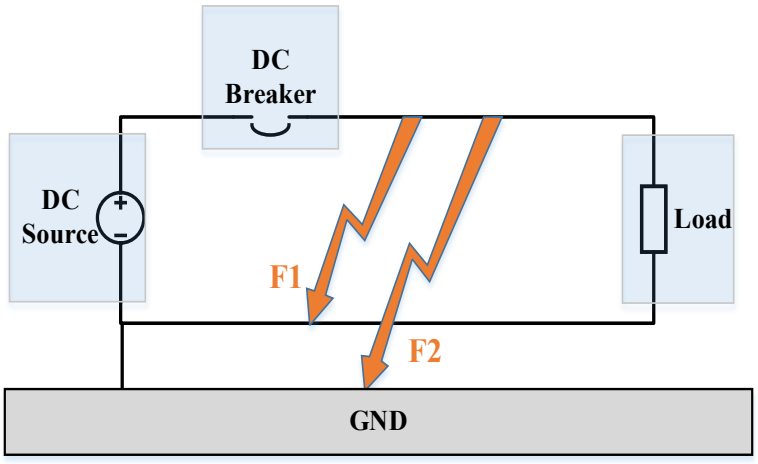

Figure 5. Short circuit faults.

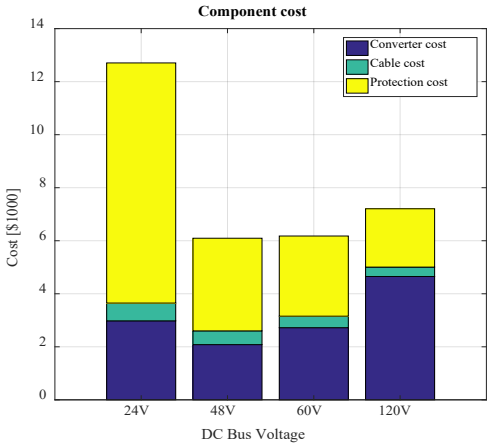

Figure 6. Total component cost at each voltage level.

6. Results and Discussion

Simulations were conducted using real data for PV, loads, and converter efficiency curves. Four voltage levels were used for the DC distribution, and at each voltage level, the DC-RNG was simulated with and without batteries. Simulations were performed using annual data, which means that different weather conditions' impacts are included in the study.

The DC-RNG's efficiency for different voltage levels is shown in Figure 7. At each voltage, two bars represent the efficiency of the DC-RNG$_{PV}$ and DC-RNG$_{PV\text{-}B}$. The results in Figure 7 indicate that the efficiency of the DC-RNG$_{PV}$ increases as the voltage level increases from 24 V to 60 V, but it drops from 60 V to 120 V DC-RNG$_{PV}$. The DC-RNG$_{PV}$ with 60 V DC distribution is more efficient than other voltage levels, and 24 V distribution is the least efficient one. Compared to DC-RNG$_{PV}$, efficiencies of the DC-RNG$_{PV\text{-}B}$ increased at 24 V, 48 V, and 120 V distribution voltages; however, at 60 V distribution voltage, DC-RNG$_{PV\text{-}B}$'s efficiency dropped with the addition of batteries. In general, adding batteries to a DC-RNG may not result in efficiency improvement.

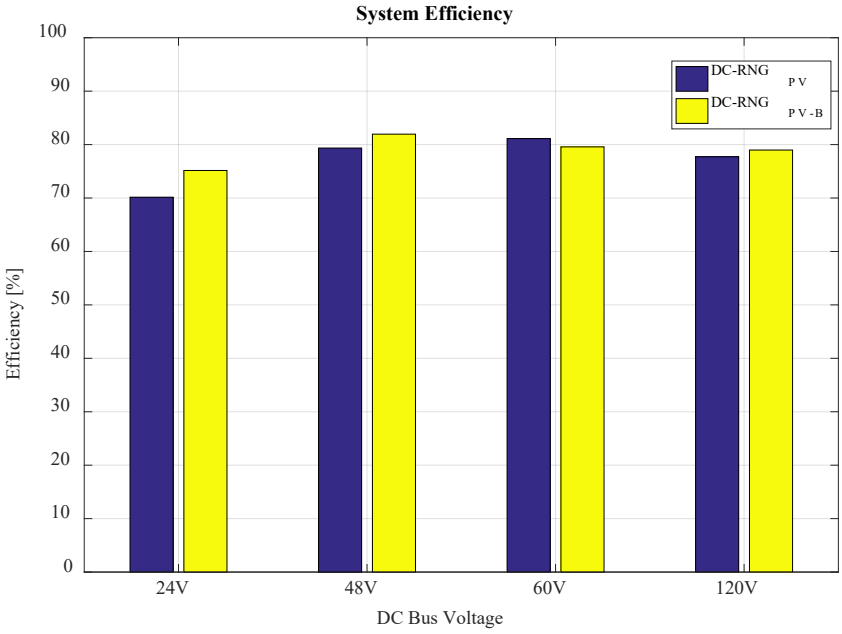

Figure 7. The DC-RNG's efficiency for different voltage levels without and with batteries.

To identify the power loss sources, the loss breakdown of the DC-RNG$_{PV}$ and DC-RNG $_{PV\text{-}B}$ are shown in Figure 8a and 8b, respectively. Figure 8a represents the amount

of energy loss in converters and wires to the total energy consumed by the DC-RNG. Figure 8a indicates that at high voltages, the wire loss decreases dramatically, but the loss of the converters does not follow a consistent pattern. Figure 8b represents the amount of energy dissipated in converters, wires, and batteries to the total energy consumed by the DC-RNG. The converter loss is the dominant source of power loss in the DC-RNG$_{PV}$, and in the DC-RNG$_{PV\text{-}B}$, either converter loss or chemical loss is the dominant source of power loss, depending on the voltage level.

Among the different voltage levels in the DC-RNG$_{PV}$, 24 V system is the least efficient due to high converter and wiring losses. By contrast, the 60 V system is the most efficient mainly because of the lower converter loss. Compared to DC-RNG$_{PV}$, in the DC-RNG$_{PV\text{-}B}$, converter loss decreases at each voltage level, but adding batteries introduces the battery chemical loss to the nanogrid. The wiring loss follows the same pattern in the DC-RNG$_{PV}$ and DC-RNG$_{PV\text{-}B}$.

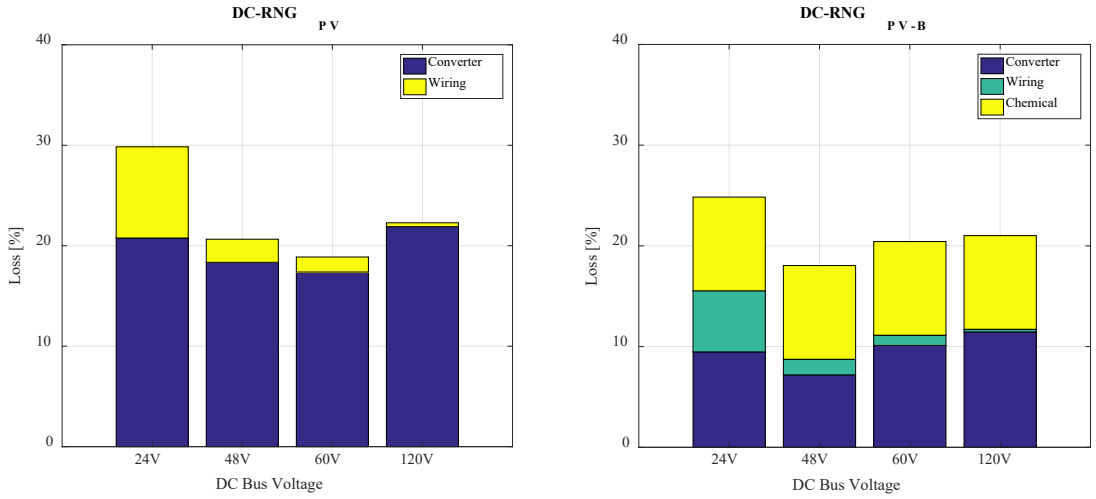

Figure 8. DC-RNG loss breakdown: (**a**) without batteries, (**b**) with batteries.

Based on Figure 8, the converter loss is the dominant source of power loss in the DC-RNG$_{PV}$. By examining the converter loss breakdown in the DC-RNG$_{PV}$ in Figure 9a, it is obvious that the AC–DC converter is the dominant source of power loss among converters. For the DC-RNG$_{PV\text{-}B}$, as shown in Figure 9b, either the AC–DC converter or MPPT CC converter is the dominant source of power loss.

Previous results are given for a battery bank capacity of 24 kWh and changing battery capacity affects the efficiency of a DC-RNG. In Figure 10a, the efficiency of the DC-RNGs is shown by sweeping the battery capacity from 2.4 kWh to 36 kWh. As shown in this figure, by increasing battery capacity, efficiency of the DC-RNGs changes significantly at lower capacities. At higher battery capacities, efficiencies do not change considerably. According to Figure 9, the AC–DC converter loss accounts for a significant portion of the total loss. Figure 10b shows that at low capacities, the loss of the AC–DC converters drop significantly by increasing the battery capacity, but they almost are constant at higher capacities. At each voltage level, the AC–DC converter operates when the DC-RNG absorbs power from or injects power to the grid. Increasing battery capacity reduces the power transferring in both directions, but due to the limited PV generation, the stored battery energy is not sufficient for the DC-RNG$_{PV\text{-}B}$ operation during nights, and the DC-RNG$_{PV\text{-}B}$ absorbs power from the grid. Therefore, choosing a high battery capacity for the DC-RNG is not advisable.

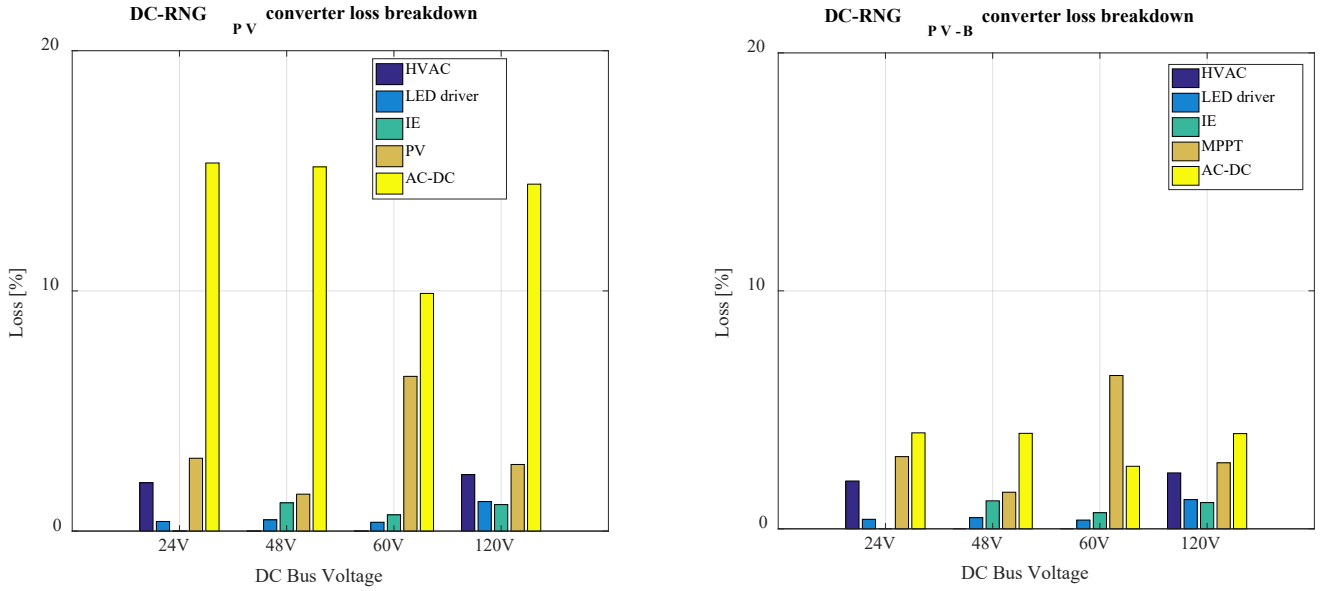

(**a**) (**b**)

Figure 9. Converter loss breakdown: (**a**) without batteries, (**b**) with batteries.

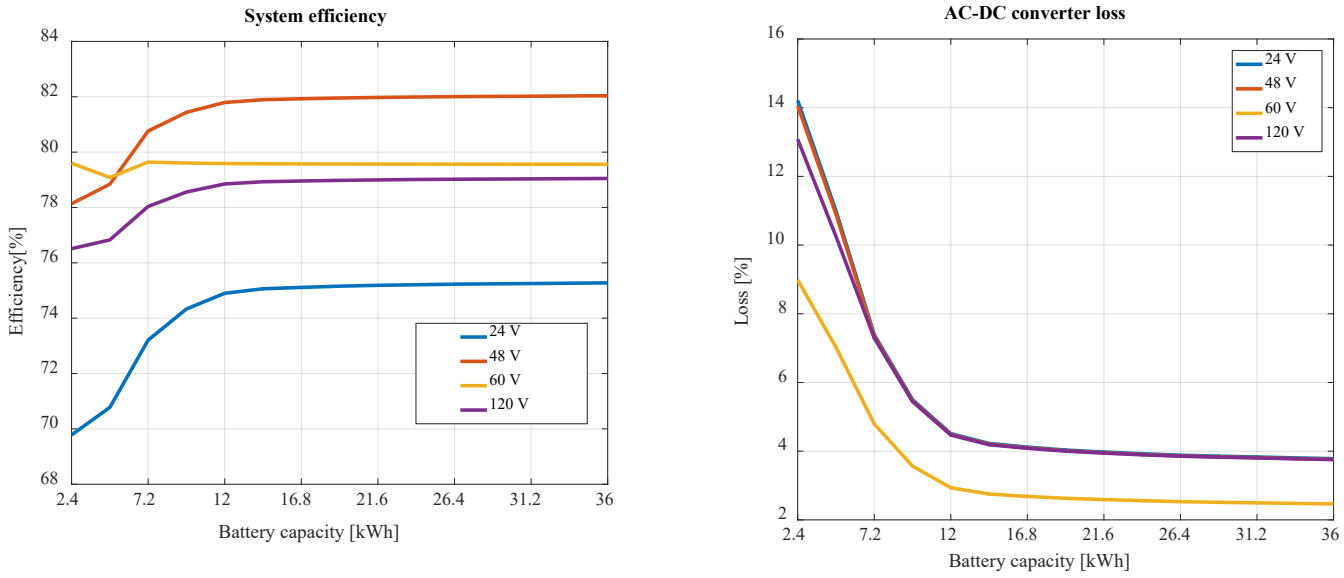

(**a**) (**b**)

Figure 10. Efficiency of DC-RNG and AC–DC converter loss by sweeping battery capacity: (**a**) DC-RNG efficiencies, (**b**) AC–DC converter loss.

Using the battery capacity of 24 kWh, SoC of the battery bank, PV generation, and load profiles are shown in Figure 11. Figure 11a shows a five-day period of the SoC, PV, and load from 100th to 105th day of a year, beginning on 1 January, during which the SoC of batteries reached 100% during daytime due to the high PV power generation and low load power. However, the SoC remained close to its minimum value during low PV generation and high load power period, as shown in Figure 11b.

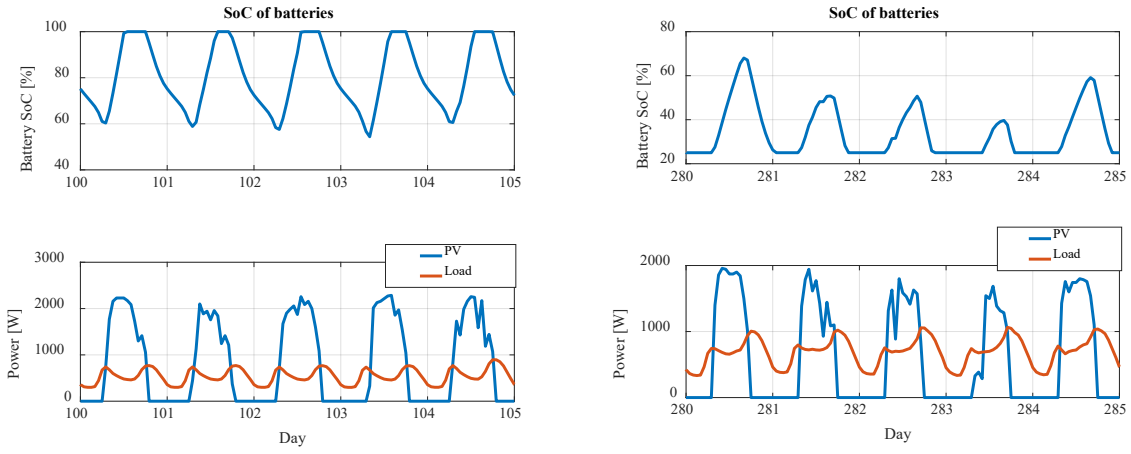

(**a**) (**b**)

Figure 11. Battery SoC and PV-load power during a five-day period: (**a**) in April, (**b**) in October.

7. Conclusions

DC voltage levels for power distribution have been investigated for years, and two voltage levels of 380 V and 48 V are commonly used in commercial buildings such as data centers. Due to different load natures in the residential sector, addressing the voltage level selection problem in DC-RNGs must be studied separately. Therefore, in this paper, voltage level selection of a gird-connected DC-RNG is studied. To include DC market-ready appliances in the study, the realistic load profiles of AC appliances were modified to DC load profiles for available appliances. The modeled DC-RNG is composed of the modified load and realistic PV generation profiles, market-ready converters' efficiency curves, and a detailed wiring diagram based on the floor plan.

Regarding the simulation results, 60 V DC-RNG$_{PV}$ was the most efficient among the studied voltages, but by adding batteries to the DC-RNG$_{PV}$, 48 V DC-RNG$_{PV\text{-}B}$ became the most efficient one. Among the studied voltage levels, 24 V distribution was the least efficient in both the DC-RNG$_{PV}$ and DC-RNG$_{PV\text{-}B}$.

To evaluate different voltage levels financially, the cost of components (converters, circuit breakers, and cables) were considered. The protection cost at 24 V DC-RNG was much higher than the cable and converter cost, and it decreased at higher voltages. The converter cost was higher than the protection and cable cost at 120 DC-RNG. 48 V and 24 V DC-RNGs yielded the least and the most component cost, respectively. The DC-RNG component cost had a minor increase from 48 V to 60 V DC-RNG. Regarding the efficiency and component cost, 48 V DC-RNG$_{PV\text{-}B}$ and 60 V DC-RNG$_{PV}$ are the best choices for a residential nanogrid with and without batteries, respectively.

Author Contributions: Conceptualization, S.H., R.R., M.F.; methodology, S.H. and P.S.; software, S.H. and R.R.; validation, M.F., and P.S.; formal analysis, S.H.; investigation, S.H.; resources, M.F. and P.S.; data curation, S.H. and R.R.; writing—original draft preparation, S.H.; writing—review and editing, R.R., M.F. and P.S.; visualization, S.H. and R.R.; supervision, M.F. and P.S.; project administration, M.F. and P.S. All authors have read and agreed to the published version of the manuscript.

Funding: This research received no external funding.

Data Availability Statement: Publicly available datasets were analyzed in this study. These data can be found here: [https://data.openei.org/submissions/153] and [https://www.nrel.gov/grid/solar-power-data.html].

Conflicts of Interest: The authors declare no conflict of interest.

Appendix A

Appendix A.1. Load Profiles

The annual average load profiles of each load category of the DC-RNG are shown in Figure A1.

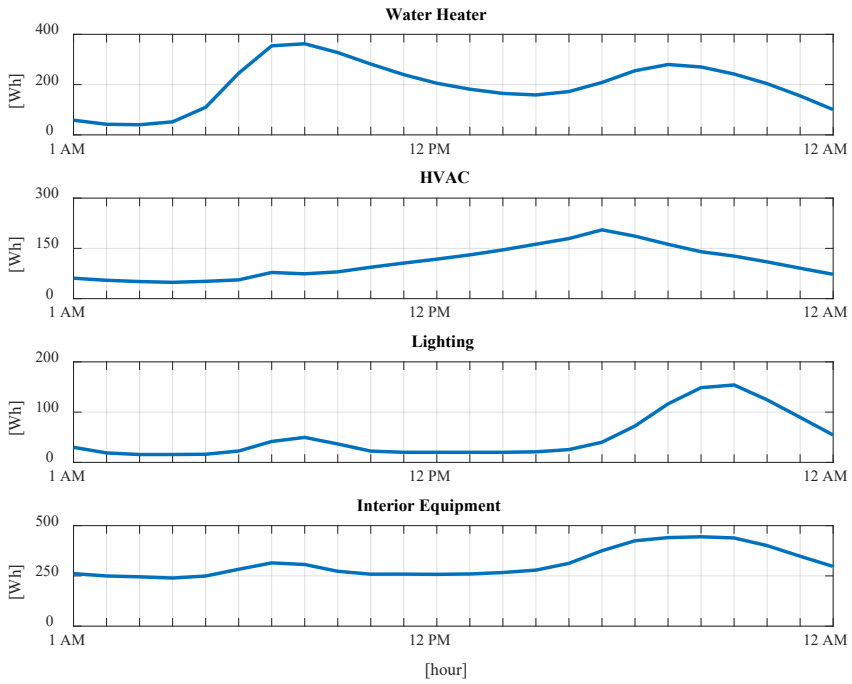

Figure A1. Average load profiles of water heater, HVAC, Lighting, and IE.

Appendix A.2. HVAC

Table A1. AC and DC HVAC specifications.

Type	Model	Cooling (BTU)	Heating (BTU)	Rated Power (W)
DC	SWWR-7.2IM	24,000	25,000	2039
AC	GSZ16-0241B	24,000	24,000	3010

Appendix A.3. IE

For a house where two people live, a 424 L (15 cu ft). refrigerator/freezer is typical. Based on the WRT106TFD energy guide manual, the minimum power consumption is 311 kWh per year and the maximum power consumption is 455 kWh per year [31]. A DC refrigerator with the same capacity consumes 200 kWh and 316 kWh per year at its minimum and maximum power usage, respectively [32]. Therefore, the AC refrigerator consumes approximately 1.5 times more power than its DC counterpart on average. Based on the data, the interior equipment consume about 1121.6 kWh per year and a typical AC refrigerator consumes 344 kWh per year. Therefore, 30.6% of IE's power is consumed by the refrigerator.

Appendix B

Efficiency curve of converters for different voltage levels are shown in Figure A2.

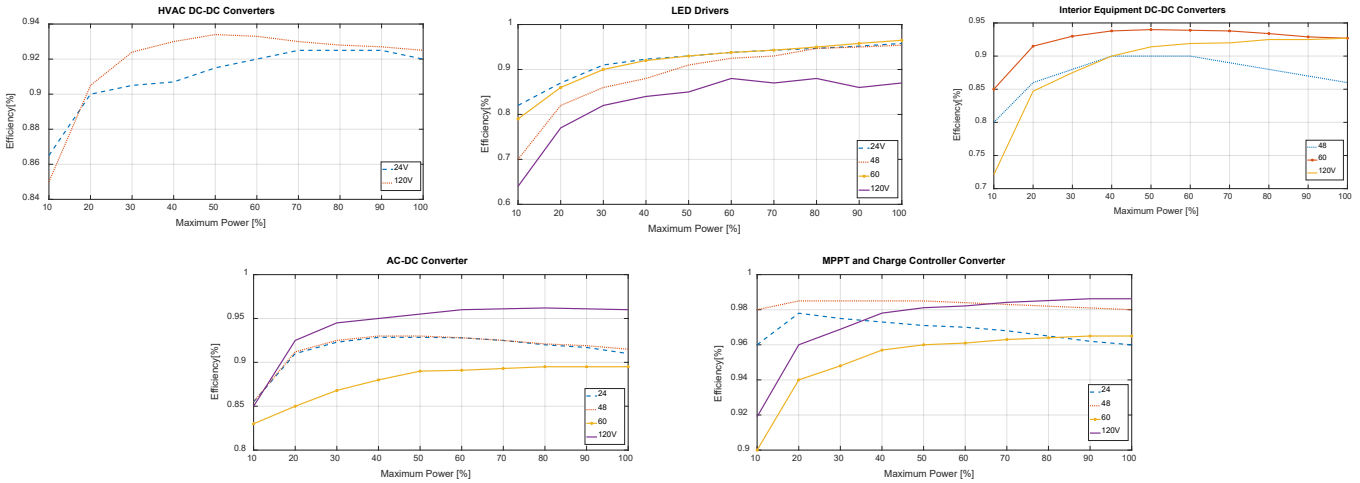

Figure A2. Efficiency curves of the converters.

Appendix C

Appendix C.1. PV Generation Profile

The daily averaged PV power generation profile is shown in Figure A3.

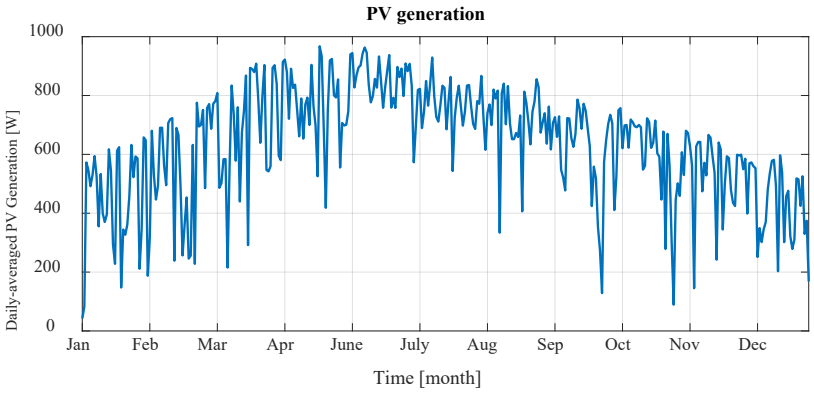

Figure A3. Annual PV power generation.

Appendix C.2. Battery Size Impact on BDT and Efficiency

The efficiency and BDT of 24 V DC-RNG is shown in Figure A4. The efficiency curve in this figure reveals that increasing the battery capacity beyond 24 kWh does not increase the efficiency noticeably. Additionally, the BDT does not drop considerably in larger capacities beyond 24 kWh.

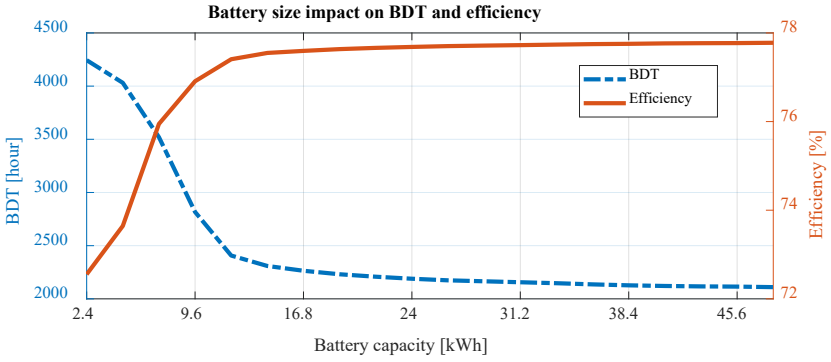

Figure A4. Battery size impact on BDT and efficiency of the DC-RNG by sweeping battery capacity from 2.4 kWh to 48 kWh.

References

1. Glasgo, B.; Azevedo, I.L.; Hendrickson, C. How much electricity can we save by using direct current circuits in homes? Understanding the potential for electricity savings and assessing feasibility of a transition towards DC powered buildings. *Appl. Energy* **2016**, *180*, 66–75. [CrossRef]
2. Gerber, D.L.; Vossos, V.; Feng, W.; Marnay, C.; Nordman, B.; Brown, R. A simulation-based efficiency comparison of AC and DC power distribution networks in commercial buildings. *Appl. Energy* **2017**, *210*, 1167–1187. [CrossRef]
3. Fotopoulou, M.; Rakopoulos, D.; Trigkas, D.; Stergiopoulos, F.; Blanas, O.; Voutetakis, S. State of the Art of Low and Medium Voltage Direct Current (DC) Microgrids. *Energies* **2021**, *14*, 5595. [CrossRef]
4. Allee, G.; Tschudi, W. Edison Redux: 380 Vdc Brings Reliability and Efficiency to Sustainable Data Centers. *IEEE Power Energy Mag.* **2012**, *10*, 50–59. [CrossRef]
5. Vossos, E.; Pantano, S.; Heard, R.; Brown, R.E. DC appliances and DC power distribution: A bridge to the future net zero energy homes. In Proceedings of the 9th International Conference on Energy Efficiency in Domestic Appliances and Lighting–EEDAL'17, Irvine, CA, USA, 13–15 September 2017.
6. Gelani, H.; Dastgeer, F.; Nasir, M.; Khan, S.; Guerrero, J. AC vs. DC Distribution Efficiency: Are We on the Right Path? *Energies* **2021**, *14*, 4039. [CrossRef]
7. Denkenberger, D.; Driscoll, D.; Lighthiser, E.; May-Ostendorp, P.; Trimboli, B.; Walters, P. *DC Distribution Market, Benefits, and Opportunities in Residential and Commercial Buildings*; Pacific Gas and Electric Company: San Francisco, CA, USA, 2012.
8. Rodriguez-Diaz, E.; Vasquez, J.C.; Guerrero, J.M. Potential energy savings by using direct current for residential applications: A Danish household study case. In Proceedings of the 2017 IEEE Second International Conference on DC Microgrids (ICDCM), Nuremburg, Germany, 27–29 June 2017; pp. 547–552.
9. Vossos, V.; Garbesi, K.; Shen, H. Energy savings from direct-DC in U.S. residential buildings. *Energy Build.* **2014**, *68*, 223–231. [CrossRef]
10. Sulaeman, I.; Chandra Mouli, G.R.; Shekhar, A.; Bauer, P. Comparison of AC and DC Nanogrid for Office Buildings with EV Charging, PV and Battery Storage. *Energies* **2021**, *14*, 5800. [CrossRef]
11. Duan, J.; Li, Z.; Zhou, Y.; Wei, Z. Study on the voltage level sequence of future urban DC distribution network in China: A Review. *Int. J. Electr. Power Energy Syst.* **2019**, *117*, 105640. [CrossRef]
12. Kaipia, T.; Sebellin, P.; Mahendru, V.; Hirose, K.; De Kesel, W.; Luber, G.; Pelta, R.; Goswami, D. Survey of market prospects and standardisation development needs of LVDC technology. *CIRED—Open Access Proc. J.* **2017**, *2017*, 454–458. [CrossRef]
13. Rodriguez-Diaz, E.; Chen, F.; Vasquez, J.C.; Guerrero, J.M.; Burgos, R.; Boroyevich, D. Voltage-level selection of future two-level LVdc distribution grids: A compromise between grid compatibiliy, safety, and efficiency. *IEEE Electrif. Mag.* **2016**, *4*, 20–28. [CrossRef]
14. Sannino, A.; Postiglione, G.; Bollen, M.H. Feasibility of a DC network for commercial facilities. In Proceedings of the 2002 IEEE Industry Applications Conference, 37th IAS Annual Meeting (Cat. No. 02CH37344), Pittsburgh, PA, USA, 13–18 October 2002; pp. 1710–1717.
15. Moussa, S.; Ghorbal, M.J.-B.; Slama-Belkhodja, I. Bus voltage level choice for standalone residential DC nanogrid. *Sustain. Cities Soc.* **2019**, *46*, 101431. [CrossRef]
16. Arunkumar, G.; Elangovan, D.; Sanjeevikumar, P.; Holm-Nielsen, J.B.; Leonowicz, Z.; Joseph, P.K. DC Grid for Domestic Electrification. *Energies* **2019**, *12*, 2157. [CrossRef]
17. Backhaus, S.N.; Swift, G.W.; Chatzivasileiadis, S.; Tschudi, W.; Glover, S.; Starke, M.; Wang, J.; Yue, M.; Hammerstrom, D. *DC Microgrids Scoping Study. Estimate of Technical and Economic Benefits*; Los Alamos National Lab.(LANL): Los Alamos, NM, USA, 2015. [CrossRef]
18. Azaioud, H.; Claeys, R.; Knockaert, J.; Vandevelde, L.; Desmet, J. A Low-Voltage DC Backbone with Aggregated RES and BESS: Benefits Compared to a Traditional Low-Voltage AC System. *Energies* **2021**, *14*, 1420. [CrossRef]
19. Gerber, D.L.; Liou, R.; Brown, R. Energy-saving opportunities of direct-DC loads in buildings. *Appl. Energy* **2019**, *248*, 274–287. [CrossRef]
20. Prabhala, V.A.; Baddipadiga, B.P.; Fajri, P.; Ferdowsi, M. An Overview of Direct Current Distribution System Architectures & Benefits. *Energies* **2018**, *11*, 2463. [CrossRef]
21. Wilson, E. Commercial and Residential Hourly Load Profiles for all TMY3 Locations in the United States. In *U.S. Department of Energy Open Data Catalog*; U.S. Department of Energy: Washington, DC, USA, 2014.
22. Garbesi, K.; Vossos, V.; Shen, H. *Catalog of DC Appliances and Power Systems*; LBNL-5364E; Lawrence Berkeley National Laboratory: Berkeley, CA, USA, 2011.
23. Heidari, M.; Majcen, D.; van der Lans, N.; Floret, I.; Patel, M.K. Analysis of the energy efficiency potential of household lighting in Switzerland using a stock model. *Energy Build.* **2017**, *158*, 536–548. [CrossRef]
24. McBride, B. Comparing LED vs. CFL vs. Incandescent Light Bulbs. Available online: https://www.viribright.com/lumen-output-comparing-led-vs-cfl-vs-incandescent-wattage/ (accessed on 6 June 2021).
25. Guide to Home Heating and Cooling. 2010. Available online: https://www.energy.gov/sites/prod/files/guide_to_home_heating_cooling.pdf (accessed on 6 June 2021).
26. DC WATER HEATING ELEMENTS. Missouri Wind and Solar. Available online: https://windandsolar.com/dc-water-heating-elements/ (accessed on 6 June 2021).

27. N. R. E. L. (NREL). Solar Power Data for Integration Studies. 2006. Available online: https://www.nrel.gov/grid/solar-power-data.html (accessed on 6 June 2021).
28. Habibi, S.; Rahimi, R.; Shamsi, P.; Ferdowsi, M. Efficiency Assessment of a Residential DC Nanogrid with Low and High Distribution Voltages Using Realistic Data. In Proceedings of the 2021 IEEE Green Technologies Conference (GreenTech), Denver, CO, USA, 7–9 April 2021; pp. 574–579. [CrossRef]
29. Circuit Breakers for Direct Current Applications up to 380 V DC: Choosing and Implementing Protective Devices. Available online: https://www.se.com/ww/en/download/document/CA908061E/ (accessed on 6 June 2021).
30. Deep Cycle AGM Battery 12 Volt 100Ah. Available online: https://www.renogy.com/ (accessed on 6 June 2021).
31. Available online: https://www.whirlpool.com/ (accessed on 6 June 2021).
32. Available online: https://www.thecabindepot.com/ (accessed on 6 June 2021).